Supplemental Information

Sequence and biochemical analysis of vaccinia virus A32 protein: Implications for in vitro stability and coiled-coil motif mediated regulation of the DNA-dependent ATPase activity

Uma Ramakrishnan†, Tanvi Aggarwal†, and Kiran Kondabagil[*],

Department of Biosciences and Bioengineering, Indian Institute of Technology Bombay, Powai, Mumbai, India

†: Equal contribution

*: Corresponding author: kirankondabagil@gmail.com, kirankondabagil@iitb.ac.in

| Gene	Vector	Forward primer 5'→3'	Reverse primer 5'→3'
A32L	pET41a	ATCTA<u>CATATG</u>ATGAATTGTTTCCAAGAAAAACAA (NdeI)	ACAATA<u>CTCGAG</u>TGATGATACATTTTTTGACGAC (XhoI)
	pET22b	ATAACA<u>CCATGG</u>GCATGAATTGTTTCCAAGAAAAACAA (NcoI)	ACAATA<u>CTCGAG</u>TGATGATACATTTTTTGACGAC (XhoI)
	pGEX-6P-1	ATCTG<u>GGATCC</u>ATGAATTGTTTCCAAGAAAAACAA (BamHI)	ACTTA<u>GTCGAC</u>TTATGATGATACATTTTTTGACGA (SalI)
	pET32b and pET32b-HRV3C	ATCCG<u>CCATGG</u>GCATGAATTGTTTCCAAGAAAAACAATTT (NcoI)	ACAATA<u>CTCGAG</u>TGATGATACATTTTTTGACGAC (XhoI)
	pFastBac1	ATCTG<u>GGATCC</u>ATGAATTGTTTCCAAGAAAAACAA (BamHI)	ACAATA<u>CTCGAG</u>TTATGATGATACATTTTTTGACGAC (XhoI)
A32L$_{CO}$	pET28a	ATCTG<u>CCATGG</u>GCAACTGTTTCCAGGAAAAACAG (NcoI)	ACAATA<u>AAGCTT</u>ACTACTAACATTTTTGCTGCTGC (HindIII)
A32LΔ20C	pET41a	ATCTA<u>CATATG</u>ATGAATTGTTTCCAAGAAAAACAA (NdeI)	ATCT<u>AAGCTT</u>TTCTAATATAGCGTTTAGATTCTTTTTCATGTG (HindIII)

Table S1. List of primers used for A32L-recombinant plasmid construction. Restriction enzyme sites are underlined

| Mutant	Overlap forward primer 5'→3'	Overlap reverse primer 5'→3'
A32L$_{K31A}$	TCTGGATCTGGA<u>GCA</u>ACTAT CTATTTA	TAAATAGATAGT<u>TGC</u>TCCAG ATCCAGA
A32L$_{L234K}$	AACATCGATATT<u>AAA</u>GTAAA TCAATATTC	GAATATTGATTTAC<u>TTT</u>AAT ATCGATGTT
A32L$_{L234K\_Q237A}$	ATCGATATT<u>AAA</u>GTAAAT<u>GC A</u>TATTCGCAC	GTGCGAATA<u>TGC</u>ATTTAC<u>TT T</u>AATATCGAT

Table S2 List of primers used for overlap PCR for construction of A32L mutants. Modified codons are underlined
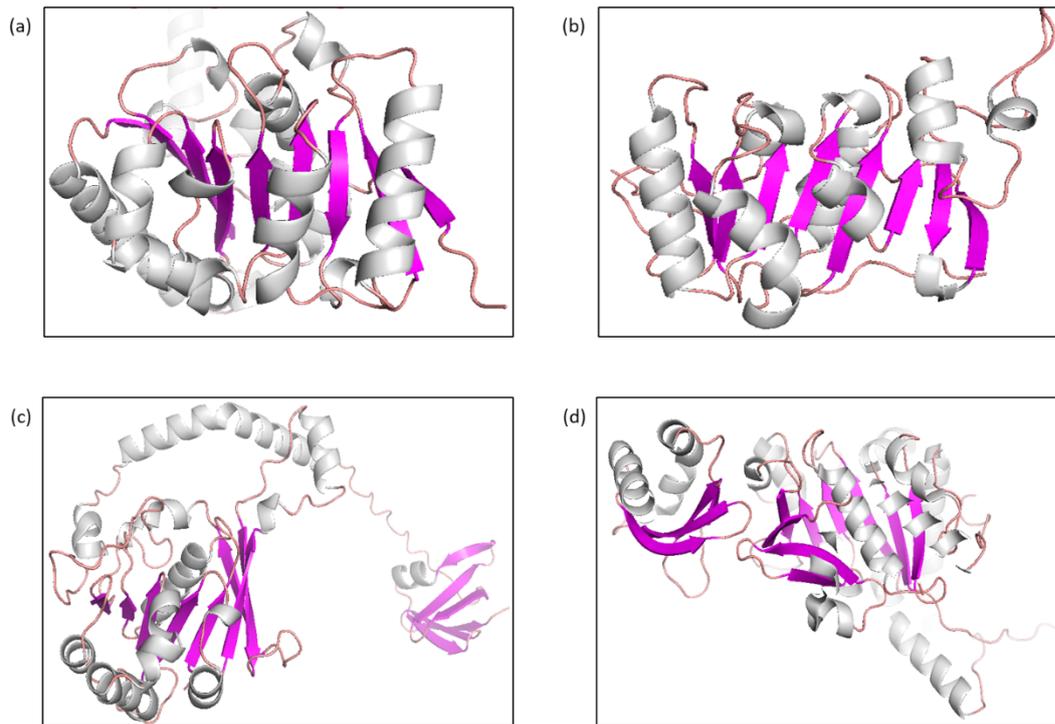
Figure S1. Alphafold predicted three dimensional structures of viral FtsK-like ATPases. (a) Predicted structure of A32 protein of vaccinia virus (accession no. YP_233037.1) representative of NCLDVs (b) Predicted structure of P9 protein of PRD1 bacteriophage (accession no. AAX45927.1) representative of membrane-containing dsDNA bacteriophages (c) Predicted structure of gp1 protein of M13 bacteriophage (accession no. NP_510893.1) (d) Custal structure of motor domain of P. aeruginosa FtsK$_{C\Delta\gamma}$ representative of ssDNA filamentous phages. Conserved β-sheet core is highlighted in pink and α-helices are shown in grey (PDB ID- 2IUT).
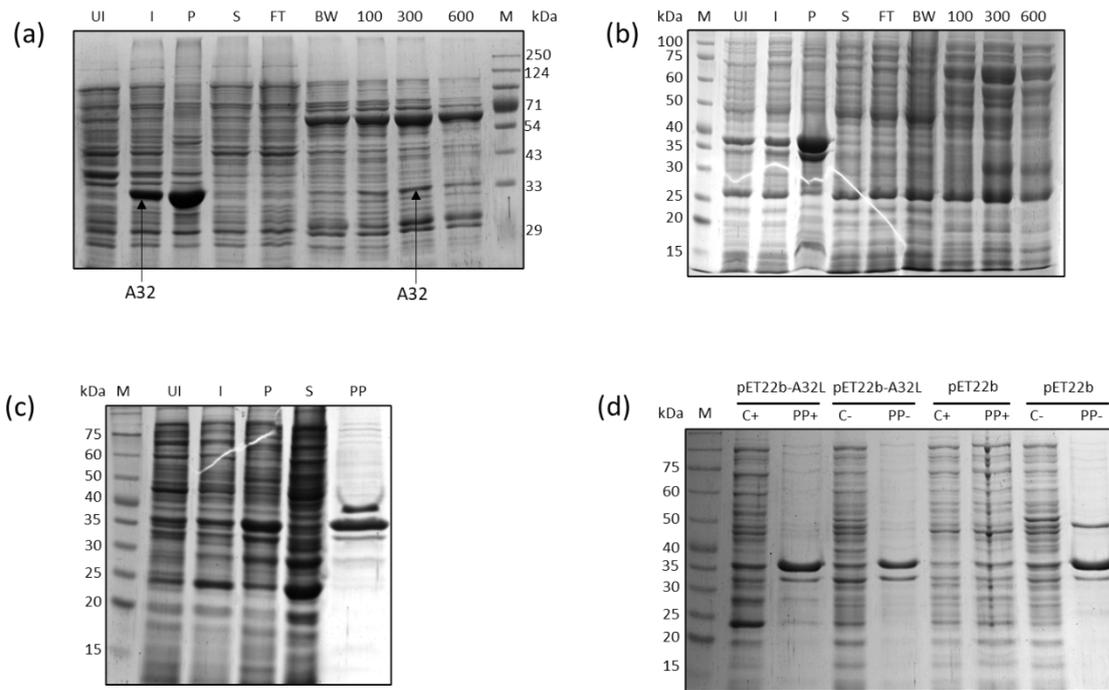
Figure S2. Expression of untagged A32 protein in *E. coli* (a) cytoplasmic expression and Ni^{2+}-NTA resin binding of A32L cloned in pET41a vector (b) cytoplasmic expression and Ni^{2+}-NTA resin binding of codon-optimised A32L$_{CO}$ cloned in pET28a vector (c) Periplasmic expression of A32L cloned in pET22b vector (d) Periplasm extraction from *E. coli* cells. Cells were transformed with pET22b plasmid or recombinant pET22b-A32 plasmid and induced (+) or not induced (-) with IPTG. M-marker; UI-uninduced cell lysate; I-induced cell lysate; P-insoluble pellet; S-soluble cytoplasmic fraction; PP-periplasmic fraction; C- cell lysate; FT-Flow through; BW1-binding buffer wash 1; BW2-binding buffer wash 2; 100, 300, and 600-elution with 100, 300, and 600 mM imidazole, respectively
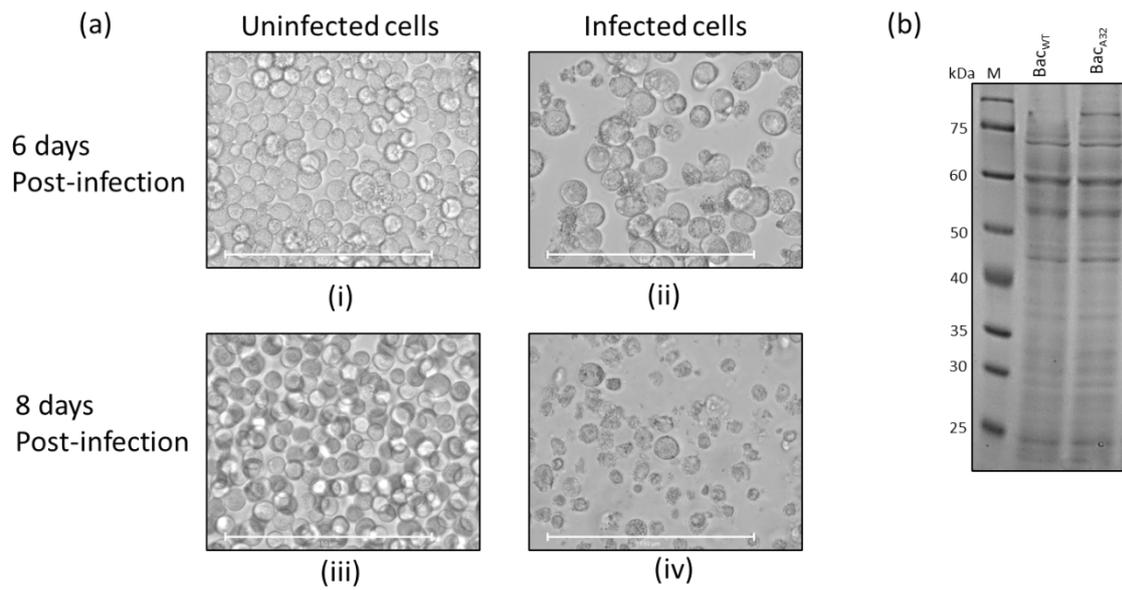
Figure S3. Expression of A32 in recombinant baculovirus-infected sf9 cells. (a) Cytopathic effects of infecting sf9 cells with recombinant A32-baculovirus. (i) uninfected cells 6 dpi (ii) infected cells 6 dpi (iii) uninfected cells 8 dpi (iv) infected cells 8 dpi. Scale bar (white): 150 μM (b) SDS-PAGE analysis of sf9 cell lysate infected with baculoviruses. M-marker; Bac$_{WT}$-wildtype baculovirus; Bac$_{A32}$-recombinant baculovirus containing A32L gene
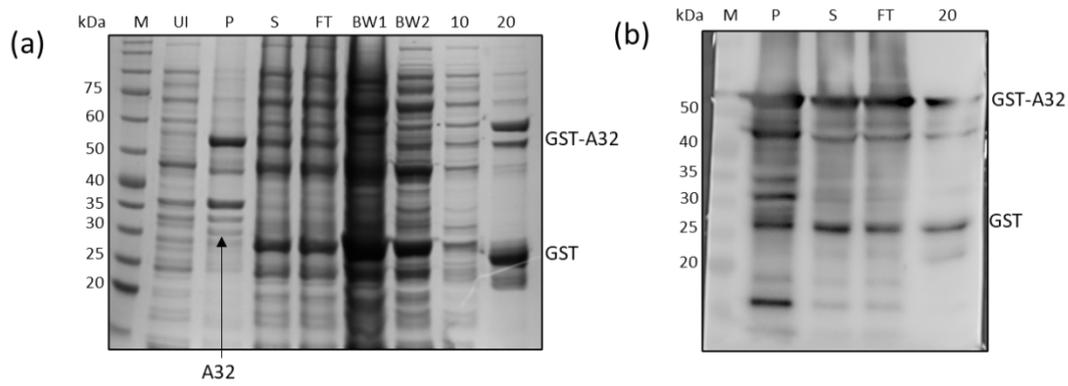
Figure S4. Expression of GST-tagged A32 in *E. coli* cytoplasm (a) Expression and glutathione Sepharose bead binding of A32L cloned in pGEX-6P-1 vector (b) Western blot with anti-GST antibody. M-marker; UI- uninduced cell lysate; I-induced cell lysate; P-insoluble pellet; S-soluble protein supernatant; FT-unbound flow-through; BW1-binding buffer wash 1; BW2-binding buffer wash 2; 10 and 20-elution with 10 and 20 mM reduced glutathione, respectively
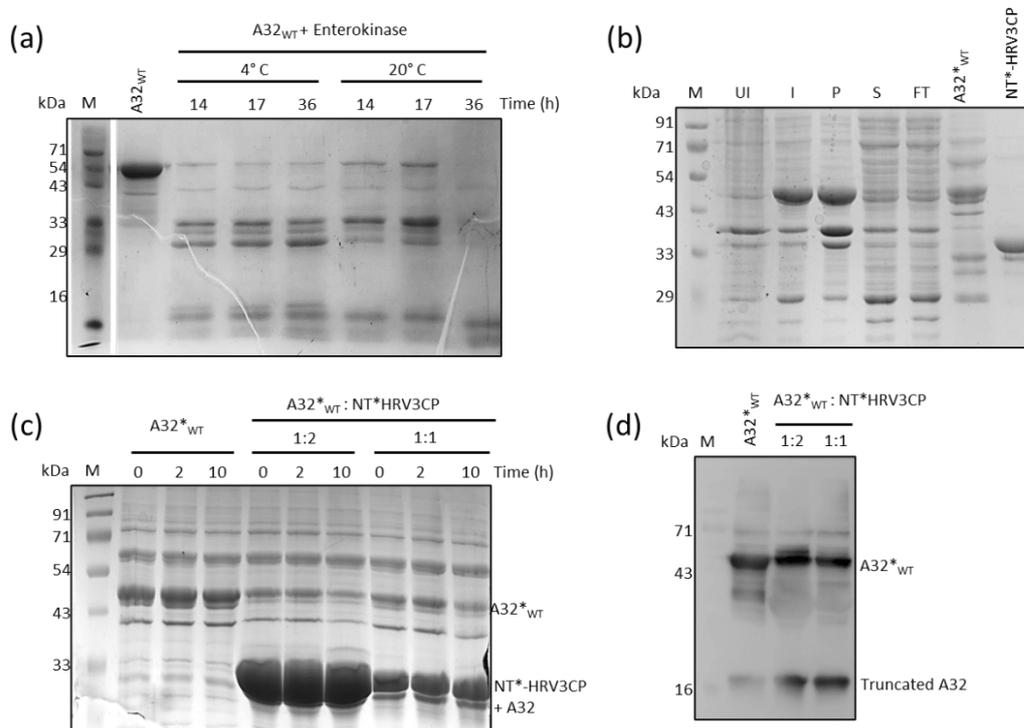
Figure S5. Removal of thioredoxin tag of A32 (a) Cleavage of thioredoxin tag by enterokinase treatment. Thioredoxin tagged wild type A32 (A32$_{WT}$) was incubated with enterokinase at 4°C and 20°C for 14, 17, and 36 h (b) Expression and purification of A32*$_{WT}$ cloned in pET32b-HRV3C plasmid. M-marker; UI- uninduced cell lysate; I-induced cell lysate; P-insoluble pellet; S-soluble protein supernatant; FT-unbound flow-through; A32*$_{WT}$-partially purified by Ni^{2+} NTA chromatography; NT*-HRV3CP-purified protease (c) Cleavage of thioredoxin tag by NT*-HRV3CP treatment. A32*$_{WT}$ was incubated with NT*-HRV3CP protease at 1:2 and 1:1 wt/wt ratio for 0, 2 and 10 h at 4°C. (d) Western blot of A32*$_{WT}$ treated with protease for 10 h using anti-A32 immune sera
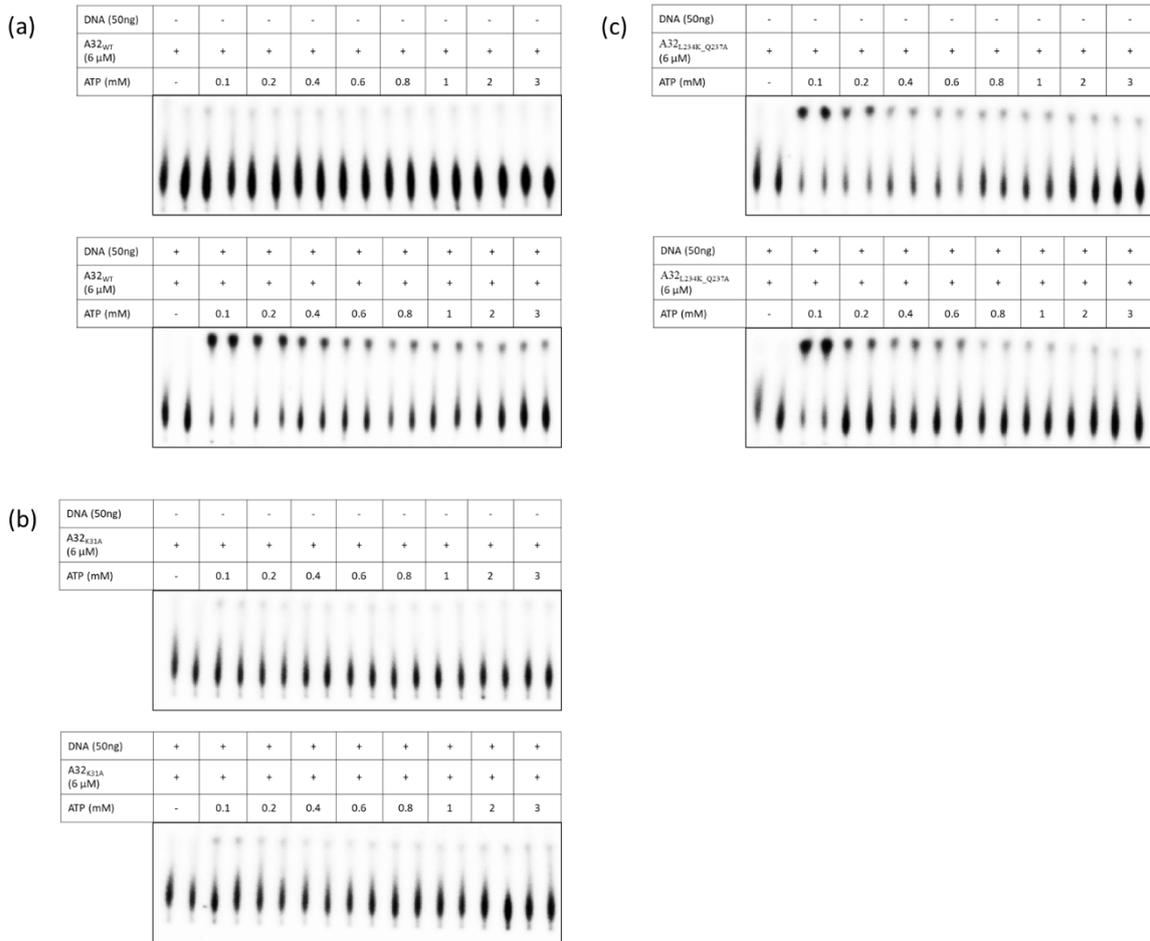
Figure S6. Autoradiographs of steady-state kinetics in the absence or presence of DNA with (a) A32$_{WT}$, (b) Walker A motif mutant A32$_{K31A}$ and (c) coiled coil motif mutant A32$_{L234K\_Q237A}$